Regional Studies in Marine Science 97 (2026) 104950

Contents lists available at ScienceDirect

Regional Studies in Marine Science

journal homepage: www.elsevier.com/locate/rsma

Trends in the relative sea level rises in French Polynesia for coastal submersion assessment from the comparative analysis of GLORYS and tide gauges / GNSS data

Bernard Ducarme [a], Marania Hopuare [b], Xianjie Li [c], Keitapu Maamaatuaiahutapu [b], Jean-Pierre Barriot [b,d,*]

[a] Catholic University of Louvain, Georges Lemaître Centre for Earth and Climate Research (ELI), Louvain-la-Neuve 1348, Belgium
[b] Geodesy Observatory of Tahiti, University of French Polynesia, Faa'a 98702, French Polynesia
[c] GNSS Research Center, Wuhan University, Wuhan 430079, China
[d] State Key Laboratory of Information Engineering in Surveying, Mapping, and Remote Sensing (LIESMARS), Wuhan University, Wuhan 430079, China

ARTICLE INFO

Keywords:
Tide Gauges
Sea level variations
Vertical land motions
GNSS
GLORYS
French Polynesia

ABSTRACT

In this study, we performed a comparative analysis, on different sites in French Polynesia, between 11 years of Tide Gauge (TG) and GNSS data and the 27 years of gridded sea level data from GLORYS (GL). The TG data provide Relative Sea Level variations (ΔRSL), while the GNSS provide Vertical Land Motions (VLM) and GL Absolute Sea Level Variations (ΔASL), at six sites (Papeete, Vairao, Rikitea, Tubuai, Makemo, and Rangiroa). In both data sets (TG and GL records), we found all the frequencies associated with climate indicators like the Interdecadal Pacific Oscillation (IPO), the Pacific Decadal Oscillation (PDO), and the El Niño Southern Oscillation (ENSO). A regional difference is found between a Northern group (TGs from the Society and Tuamotu archipelagos) and a Southern group (TGs from the Gambier and Austral islands). A strong signal of the IPO is detected at the Tubuai TG (Austral Islands), this signal could blur the secular trend. The main conclusions of this paper are: a) the inter-annual IPO variability is the only phenomenon affecting the ΔASLGL determination on the 27-year long GL series; b) due to the inter-annual variability, the 11-year time span of TG records is too short to determine reliable long-term ΔRSLTG trends; c) The subtraction of GL data from TG data, which eliminates the common inter-annual variability, provides a proxy for the determination of VLMTG, as -VLM = ΔRSL − ΔASL and the VLMTG are reliable when compared to the VLM derived from GNSS data records; d) reliable ΔRSL= ΔASLGL-VLMTG trends are obtained from the combination of TG and GL data. ΔRSL values around 2.2 mm/yr are obtained at Vairao and Rangiroa. For the Southern group, much larger values are observed due mainly to the contribution of IPO. After correction we get 2.45 mm/yr at Rikitea and 3.33 mm/yr at Tubuai.

1. Introduction

The sea level rise is of great concern everywhere in the world (Martínez-Asensio et al., 2019), and its determination requires a robust and advanced data modelling combining satellite and ground-based data (Adebisi et al., 2021; He et al., 2025; Ansari et al., 2024; Ansari, 2025).

In French Polynesia (FP, South Pacific), the Absolute Sea Level variations (ΔASL), measured by satellite altimetry, do not directly map the risks of sea flooding to populations, since the land subsidence is not considered. Indeed, most of the islands are subject to such land subsidence (Fadil et al., 2011; Oelsmann et al., 2024) because many of them are geologically young and have not yet reached the isostatic equilibrium with the underlying Earth's mantle. In contrast, Tide Gauges (TGs) measure Relative Sea Level variations (ΔRSL) with respect to the TG benchmarks on the ground, which is the real estimation of this hazard. The direct determination of the Vertical Land Motion (VLM) through collocated GNSS observations at TG sites provides an alternative way to determine ΔRSL, as the relation between the three quantities is simply:

$$\Delta RSL = \Delta ASL - VLM. \quad (1)$$

Inversely, the association of altimetry and TGs measurements provides a proxy (Cazenave et al., 1999; Kuo et al., 2004; Wöppelmann and

* Corresponding author at: Geodesy Observatory of Tahiti, University of French Polynesia, Faa'a 98702, French Polynesia.
E-mail address: jean-pierre.barriot@upf.pf (J.-P. Barriot).

https://doi.org/10.1016/j.rsma.2026.104950
Received 2 December 2025; Received in revised form 9 March 2026; Accepted 24 March 2026
Available online 27 March 2026

Marcos, 2012) of the VLM, as:

$$VLM = \Delta ASL - \Delta RSL. \quad (2)$$

These two equations are the backbone of this study.

Seven geodetic tide gauges (i.e. with collocated GNSS receivers) are currently operating in French Polynesia (Table 1 and Fig. 1). The analysis (over the period 2006–2021) of the data records has been published in previous works (Barriot et al., 2023; Ducarme et al., 2023; Li et al., 2024) except for the Papeete TG.

Our goal in this paper was to perform comparisons between TG/GNSS data and a totally different reference source to assess the reliability of our determinations of relative sea level rise and land subsidence in French Polynesia. The reference source of choice should have been, at first sight, climate-oriented altimetric grids like the CNES/CLS Sea Level Anomalies (SLA) grid available from the Copernicus Climate Change Service (C3S, CMEMS 2024b; other similar grids are available on this website), which is presented as the state-of-the-art, climate-oriented dataset of SLA with a 0.25° resolution. But we have chosen as a reference source the global ocean physical reanalysis (GLORYS, version 12V1) of the altimeter-level gridded time series (SSH, Sea Surface Heights), provided by the E.U. Copernicus Marine Service Information (CMEMS 2024a). GLORYS is a global ocean eddy-resolving (1/12° horizontal resolution, 50 vertical levels) reanalysis covering almost all the altimetry data records (1993 onward) with a one-day time resolution (Fig. 1b). We preferred to use the GLORYS grid because of its twice-higher spatial resolution than the C3S grids and also because we were mostly interested in characterizing regional ocean dynamical processes on inter-annual time scales. Climate-oriented grids, by essence, filter out these local effects, and their filtering might not be coherent with our in-house filtering applied to our TG/GNSS data on a regional scale. For tiny and long-term trends in short series, this is of the utmost importance. Moreover, Dynamic Atmospheric Correction (DAC) must be put back into the SLA datasets to obtain sea level signals that can be compared to TG observations, adding another layer of complexity and possible additional discrepancies. Let us finally note that astronomical tides have been removed from both GLORYS and C3S grids.

In French Polynesia, the fluctuations of the modelled sea level trends from the GLORYS grid are well below one mm/yr, without any specific geographical pattern to be seen (see Fig. 15 C in Lellouche et al., 2021). In the following sections of this paper, we will study the characteristics of the GL time series in connection with the known oceanographic signals. This analysis will be used to optimize the determination of the secular trend in the GL series (ΔASL). Then, the TG/GNSS data are compared with the GL data. Eq. (2) is used to determine VLM by subtracting TG-derived ΔRSL values from GL-derived ΔASL values. In our case, a global adjustment as in Kuo et al. (2004) of VLM for all the stations is not relevant, as the different islands have different tectonic evolution. VLM is linked to the age of the island as a volcano (Huppert et al., 2020). ΔRSL values are finally recomputed at each station using Eq. (1), providing an evaluation of the sea level rise with respect to the TG benchmarks; that is the real assessment of the submersion risk.

Fig. 1

2. Spectral analysis of GLORYS ΔASL and Tide Gauge ΔRSL time series

For this study, we processed the residuals of the tide analysis from the original TG data using the ET34-ANA-V80 software (Schüller, 2017). The tide signal is thus removed from the data. Details of the procedure can be found in Ducarme et al. (2023). As the GL ΔASL data are available at a daily sampling rate, it was necessary to down-sample the hourly sample rate of the TG raw ΔRSL data. To avoid aliasing, the decimation was performed after application of an appropriate low-pass Fourier filter (Schüller, 2017), with a cutoff frequency of 0.88 cpd (cycles-per-day).

The GL ΔASL data (at each 12 h UT, resolution of 1/12° in latitude and longitude) cover a time span of 10,013 days, from 1993/01/01–2020/05/31. For each TG station, we selected the values from the closest GL cell (Table 1). Fig. 2 shows a striking difference between the Northern and Southern groups of stations (see Fig. 1 for the categorization of the two groups). This North-South difference could be attributed to the synoptic ocean-atmosphere circulations. French Polynesia is located within the Subtropical gyre of the South Pacific Ocean. North of Tahiti, the South Equatorial Current is flowing westward (Martinez et al., 2009) within the trade winds from the high-pressure Easter Island anticyclone and is pushing warm waters from the tropics toward the west. South of Tahiti, in the Austral and the Gambier archipelagos, the Subtropical Counter Current is transporting warm waters eastward (Martinez et al., 2009). The Subtropical Counter Current is located underneath the low-pressure South Pacific Convergence Zone. The large-scale ocean circulation in the South Pacific Ocean is strongly perturbed by ENSO (Martinez et al., 2009) as also shown below.

The correlation coefficients between the TG ΔRSL and GL ΔASL time series are larger than 0.85 for all the stations except Makemo, where the sea swell is clearly the dominant signal (Fig. 3). Subtracting GL ΔASL data from TG ΔRSL data reduces considerably the spectral amplitudes for periods larger than 70 days (up to 0.014 cpd, Fig. 4 for Vairao TG). This is observed for all TG stations.

As the inter-annual variability can hamper the determination of GL ΔASL, a careful study of the low-frequency spectrum of the GL ΔASL data is required to remove these contributions (Moreira et al., 2021), but this is also the strength of our study, as we are assessing the inter-annual variability in both the GL ΔASL and TG ΔRSL data. In the tropical Pacific

Table 1
Location of the Tide Gauge / GNSS stations in French Polynesia maintained by the Geodesy Observatory of Tahiti/ UPF and the University of Hawaii (UH). The coordinates of the center of the closest GLORYS (GL) cell are also given, as well as the distance D of the cell w.r.t. the TGs. The Papeete tide gauge is equipped with two altimetric radars (labeled R1 and R2).

No.	Station name	Archipelago	Starting date	Management	TG Coordinates	D (km)	GL coordinates (center of cell)	Identification	
								GLOSS	PSML
1	Papeete UH	Society	Jun. 2008	UH	17°31.99'S 149°34.36'W	3.6	17.5°S 149.583°W	140	1260 1397
2	Vairao	Society	Feb. 2011	UPF	17°48.35'S 149°17.7'W	5.1	17.833°S 149.333°W		2242
3	Rangiroa	Tuamotu	Feb. 2009	UPF	14°56.75'S 147°42.36'W	5.3	14.917°S 147.750°W	355	2216
4	Makemo	Tuamotu	Oct. 2013	UPF	16°37.63'S 143°34.15'W	1.5	16.75°S 143.583°W	354	
5	Rikitea UH	Gambier	Jun. 2008	UH	23°07.33'S 134°58'W	4	23.083°S 135.0°W	138	1253
6	Mangareva/Rikitea	Gambier	Mar. 2012	UPF	23°07.07'S 134°58.13'W	4.4	23.083°S 135.0°W		
7	Tubuai	Austral	Dec. 2008	UPF	23°20.50'S 149°28.53'W	3.4	23.333°S 149.500°W	356	2217

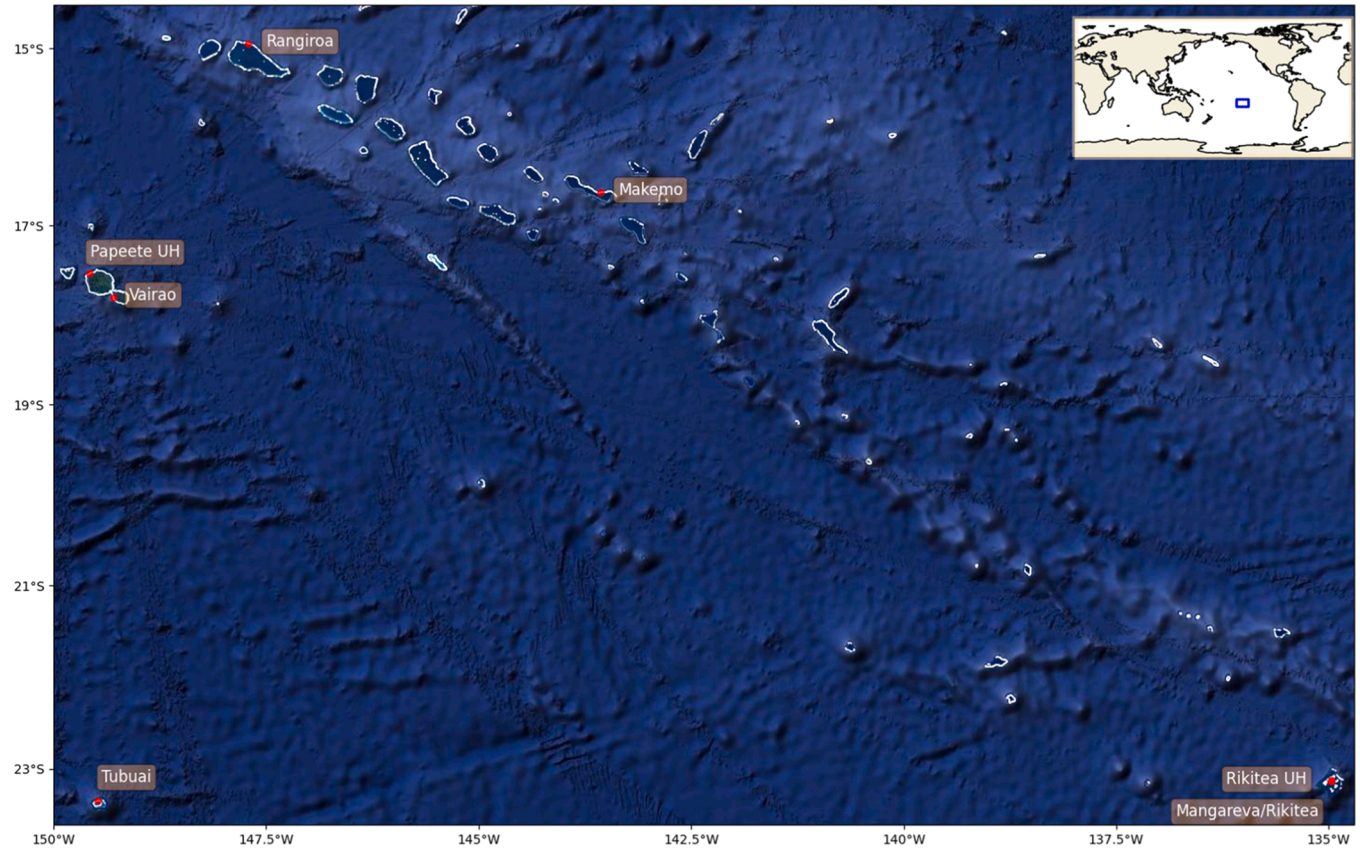

Fig. 1. a. Geographical distribution of all the Tide Gauges (TGs) over French Polynesia (red dots). See **Table 1** for exact locations. The tide gauges can be divided into two groups: a Northern group of stations (the Society Islands, with Papeete and Vairao, and the Tuamotu Archipelago, with Rangiroa and Makemo) and a Southern group (the Gambier Islands, with Mangareva/Rikitea, and Tubuai in the Austral Islands).b Global Mean Sea Surface Height above geoid (SSH) from the GLORYS12V1 product over the period of Jan 1993-Jan 2025, where the red rectangle outlines the area of interest in the paper as presented in Fig. 1a. These gridded values differ from the SSHs above the ellipsoid by the geoidal height of the selected geoid model. Both the altimeter and GPS data are referred to the WGS84 ellipsoid. As we are only concerned with the secular variations of the different quantities at specific locations, the bias between the GPS and ADT (Absolute Dynamic Topography) reference frames will not influence our results. We can therefore identify ΔASL with the ADT secular trend.

area, the El Niño Southern Oscillation (ENSO) multiyear (2–7 years period) event is the largest phenomenon. At inter-annual time scales, ENSO has a clear spatial pattern on mean sea level changes in the tropical Pacific: the mean sea level is higher than normal during El Niño events and lower than normal during La Niña events in the Eastern Pacific (Becker et al., 2012). ENSO intensity and spatial pattern diversity are the main drivers of FP inter-annual climate variability (Pagli et al., 2025). Several indexes are used to characterize the ENSO phases, such as the Multivariate ENSO Index (MEI), the Oceanic Niño Index (ONI), or the NINO34 index. By using low-pass filtered data ($T > 4$ years), Moreira et al. (2021) showed that a strong correlation (0.91) on the inter-annual signal is found between the Global Mean Sea Level variations and the MEI index. Such correlation is not directly visible in the local GL ΔASL variations, but it clearly appears in the low-frequency part of their spectra (Table 2).

We computed the amplitudes and the phases (w.r.t. an initial epoch of January 1, 1993, with lags counted positive) of the main spectral peaks, using the tidal analysis software ET34-x-v80 (Schüller, 2015, 2017). The associated RMS errors are only internal computation errors, and the errors on the derived quantities follow the rules of error propagation. In the following, we considered only the inter-annual frequency band, which might affect the determination of GL ΔASL.

The lowest inter-annual frequency in our GL ΔASL time series, a clear signal at 0.00012 cpd (22.8 years), is present in the Tubuai TG data with an amplitude of 31.1 ± 1.6 mm and in the Rikitea TG data with an amplitude of 10.95 ± 1.4 mm. This frequency is not seen in the data from stations of the Northern group. This frequency corresponds to the Interdecadal Pacific Oscillation (IPO), known as a long-term oscillation of sea-surface temperatures in the Pacific Ocean that lasts 20–30 years (Power et al., 1999; Salinger et al., 2001). It has an ENSO-like spatial signature, and it extends into the extratropics. Over the years, the phase of IPO has changed from positive during the time period 1977–1998 to negative over 1999–2013, and then again to positive since 2014 (Hua et al., 2018). IPO has wide-ranging effects on surface temperature and precipitation across various regions worldwide, as evidenced by Dai (2013), Dong and Dai (2015), Gu and Adler (2015), and Hopuare et al. (2015). Additionally, it contributes to shifts in global warming rates over decades, as indicated by Fyfe et al. (2016). More specifically, the cooling observed in the eastern Pacific since approximately 1993, due to IPO phase transition, likely plays a significant role in the recent deceleration of the global surface warming trend since the late 1990s, as suggested by studies including Dai et al. (2015) and Kosaka and Xie (2013). Using altimetry, Albrecht et al. (2019) showed that the IPO is detectable on sea surface height over the 1993–2015 period. The maximum of the IPO signal detected in the GL ΔASL data occurred in August 2012 (RMS error 1.5 month) at Tubuai and August 2013 (RMS error 5 months) at Rikitea. The beginning of 2013 corresponds to a change in IPO's phase.

The second longest period signal, with a period of 11 years (4000 days), is visible at all stations. The amplitude is close to 1 cm, except in Tubuai, where it reaches 2.5 cm. This 11-year signal is related to the Pacific Decadal Oscillation (PDO). The PDO is often described as a long-lived El Niño-like pattern of Pacific climate variability (Zhang et al.,

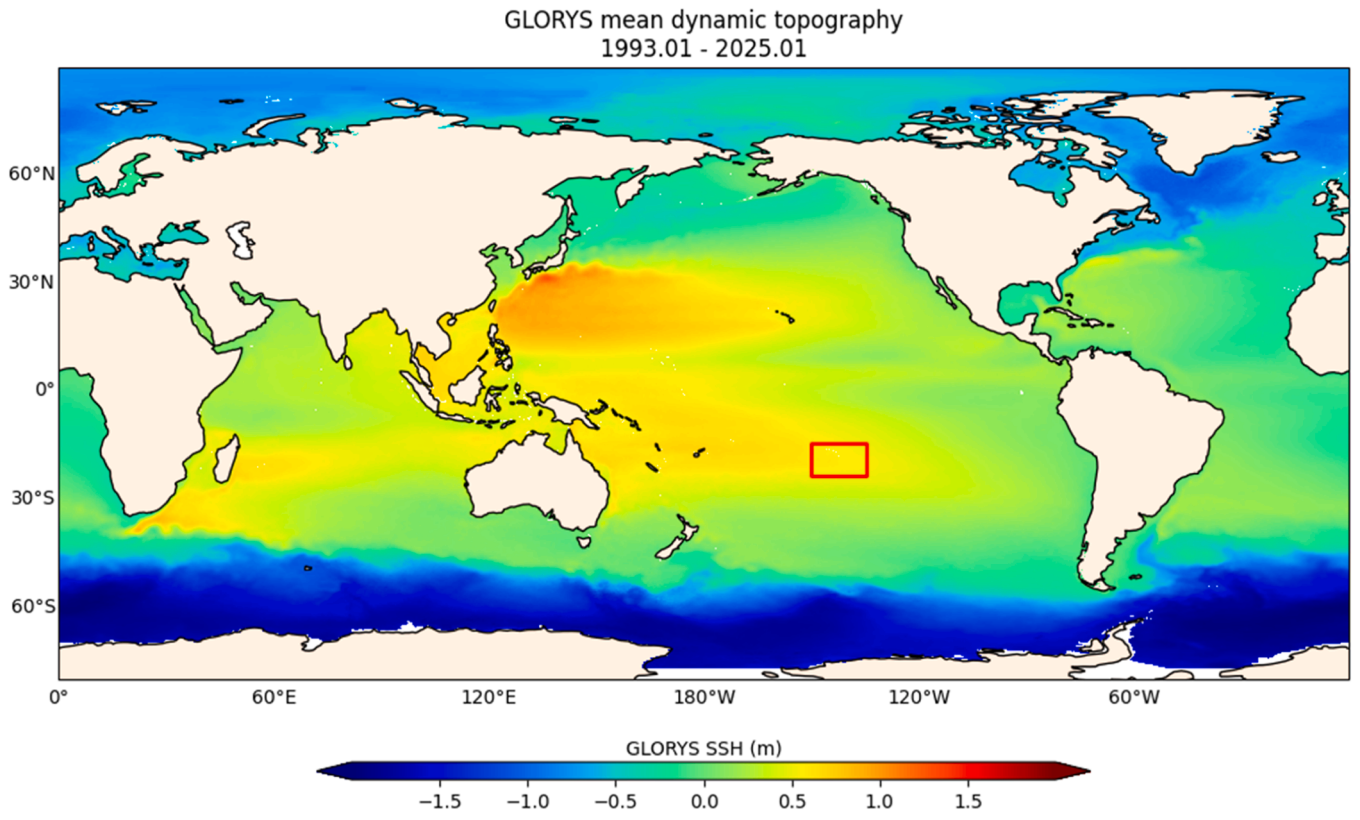

Fig. 1. (*continued*).

1997; Mantua, 2003). When Sea Surface Temperatures (SSTs) are anomalously cool inside the North Pacific basin and warm along the Pacific coast, and when sea level pressures are below average over the North Pacific, the PDO has a positive value. When these climate anomaly patterns are reversed, the PDO has a negative value. A weak mirror image of these anomalies occurs across the South Pacific. The corresponding phases of the PDO at all stations, determined from GL data (Fig. 5), show a phase opposition between the stations from the Northern group and the stations from the Southern group. Hamlington et al. (2014), who studied the contribution of the PDO to sea level trends over the Pacific Ocean from 1993 to 2010, already found such regional contrasts. In French Polynesia, the effects of PDO/IPO on sea level trends are −2 mm/yr over the Marquesas Archipelago and + 3 mm/yr over the Society Archipelago, respectively.

Periods between 2.5 and 10 years are generally associated with ENSO. A noticeable broad peak is present in the Southern group at a 5.5-year period (0.00052 cpd): Rikitea (amplitude A=11 ± 1 mm, phase φ=−179 ± 7°), Tubuai (A=10 ± 1 mm, φ=−163 ± 9°). At the two stations, the results agree within the associated RMS error. It could correspond to a harmonic of the 11-year period. However, this peak disappears in the Northern group data and is replaced by a peak corresponding to a four-year period (0.0007 cpd). Its amplitude is larger than 1 cm, with a signal-to-noise ratio larger than 20 dB. The phase is comprised between −94° and −144°, without any correlation with the longitude of the stations.

Another oscillation could be mixed with ENSO periods: the Quasi-Biennial Oscillation (QBO, Dunkerton 2003). Periods between 2 and 3 years, with an average of 28 months, are detected in data from all stations. Indeed, we found peaks at 1100 days (QBO1, 3-year) and 909 days (QBO2, 2.5- year). The amplitudes are lower in Mangareva/Rikitea and Makemo stations. Table 2 displays a comparison between the ENSO and GL spectra. All the spectral lines present in ENSO (Moreira et al., 2021, Fig. 12) are found, but there are differences between the Northern and the Southern groups.

3. Extraction of the secular trends in GLORYS ΔASL time series

If we determine the secular trend in the GL ΔASL data through a simple linear regression, the interannual periods present in the data (Section 2) may hinder the determination of the secular trend, even over the 27.5-year time series. Indeed, in the presence of a very long-period harmonic, an artificial trend may appear if the temporal extent of the dataset is not exactly a multiple of the period of this harmonic. The IPO period (23.8 years) is mainly affecting Tubuai and Rikitea, with a respective contribution to the trend at 1.16 mm/yr and 0.39 mm/yr., seriously modifying the observed ΔASL. This contamination effect is also present for other inter-annual signals but diminishes with their periods. To study this effect, we used a simultaneous determination of the secular drift represented by a Chebyshev polynomial of order one with a modeling of these long-period terms, which is also outputting the correlations between the secular and harmonic terms (Schüller, 2015, 2017). Correlations larger than 0.1 exist at frequencies ranging between 0.0005 cpd and 0.0009 cpd. Unfortunately, several harmonics show up between 2000-day and 1100-day periods (Section 2), and these harmonics can impact the determination of the secular trends. Therefore, we decided to evaluate separately all terms showing a correlation larger than 0.1 and subtract them from the original GL data set. Afterward, a good decorrelation between the secular trend and the harmonic part of the signal was obtained.

We present in Table 3 the results of two different determinations of the secular trend:

Option 1: A linear regression was used without the modeling of the inter-annual signal.

Option 2: As explained above, several long-period terms were evaluated and subtracted from the data before the determination of the secular trend. The spurious trend removed with the subtracted Long Period (LP) terms is shown in the fourth column of Table 3. As an example, the interannual signals eliminated in Rikitea based on the correlation level, excluding IPO, are PDO, PDO/2, PDO/3 and QBO2

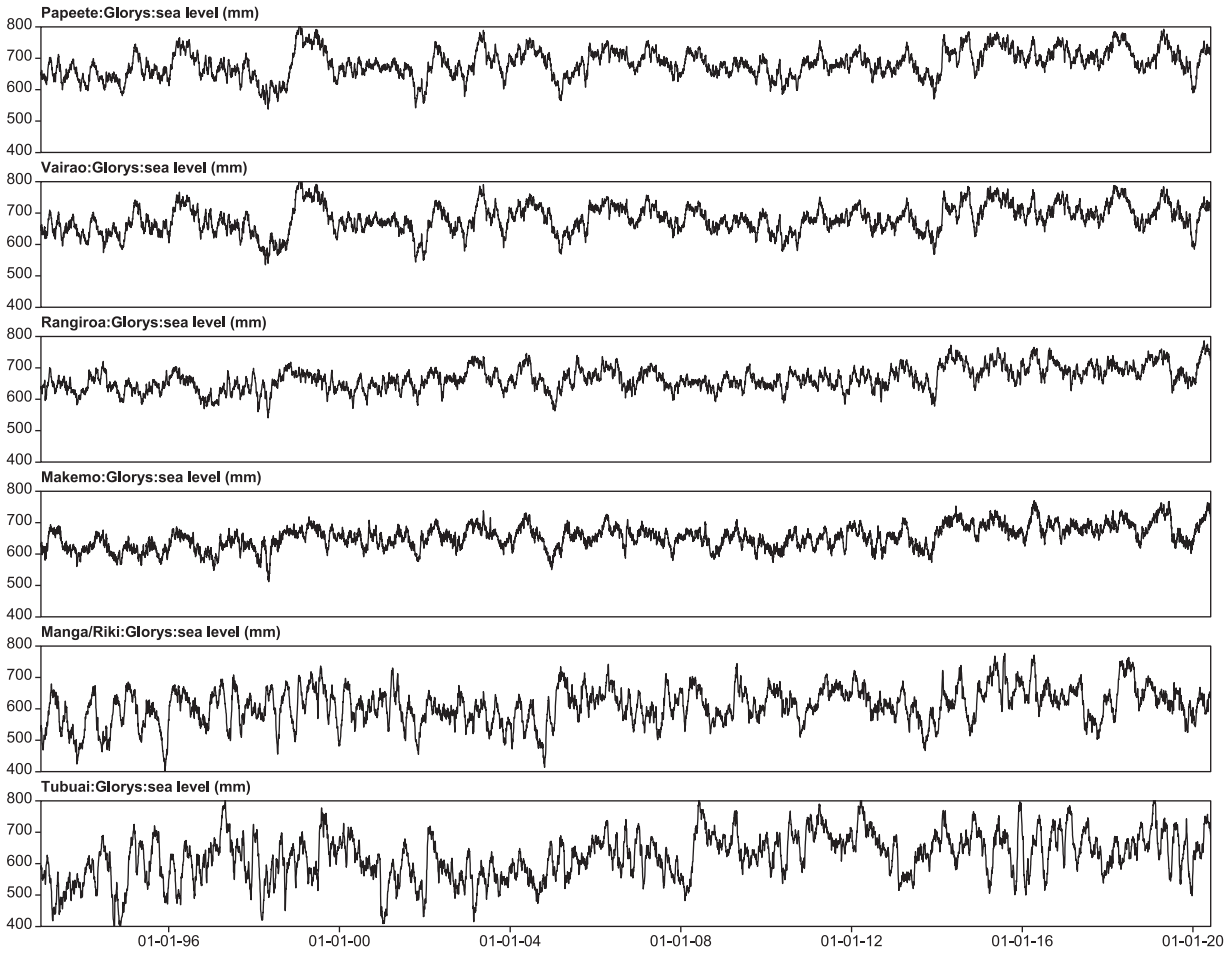

Fig. 2. GLORYS ΔASL time series close to each Tide Gauge station. From top to bottom: Papeete, Vairao, Rangiroa, Makemo, Mangareva/Rikitea, and Tubuai. The stations Papeete and Vairao are separated by around 60 km, with a correlation of 0.989 between the time series. The time series are more perturbed at short periods in Mangareva/Rikitea and Tubuai.

(Table 2).

Both methods give results that agree within the associated RMS errors, and the contribution of the removed long-period terms (fourth column of Table 3) is always negligible when the IPO contribution is not considered. In the Northern group, Rangiroa and Makemo, display very similar ΔASL trends, close to 2.27 ± 0.04 mm/yr. The values are slightly lower at Papeete TG (1.88 ± 0.05 mm/yr) and Vairao TG (1.78 ± 0.05 mm/yr), but the results agree within their RMS errors. In the Southern group, the IPO contribution should be considered. The secular trend at Tubuai is reduced to 2.63 ± 0.08 mm/yr after subtraction of the 23.8-year IPO signal from the observations. The eliminated harmonics are removing an apparent 1.28 ± 0.02 mm/yr trend, including the IPO contribution of 1.16 mm/yr. In Rikitea the subtraction of the IPO contribution reduces the secular trend from 2.21 ± 0.07 mm/yr to 1.90 +/- 0.07 mm/yr. After elimination of the climatological effects, these corrected ΔASL values could be considered as an "anthropogenic sea level rise" probably associated with the global warming. For these stations, the 27.5-year time span is obviously too short to extract a correct value of the secular trend by a linear regression.

In Table 3, we compared our results with the mean value of the results published in Li et al. (2024), Table 8). There is a good agreement, except for Papeete and Vairao TGs. The disagreement for Papeete and Vairao TGs might be due to a local anomaly in sea level height in the Society Islands, captured by the higher resolution GL model. For the Tubuai TG, the value provided by Li et al. (2024) corresponds to our uncorrected value, as they did not eliminate the IPO contribution. ΔASL trends derived from the Aviso dataset for Tubuai (3.83 mm/yr), Rangiroa (2.34 mm/yr) and Rikitea (1.92 mm/yr) confirm the agreement with ΔASL trends derived from GLORYS data and Li et al., (2024).

4. Comparison between tide gauge ΔRSL trends and GLORYS ΔASL trends

In the previous section, the trends of the GL ΔASL time series have been determined on the total time series of 27.5 years, while the TG ΔRSL data set only covers a period of 11 years (4000 days) from 2009 to 2020. It is thus important to check the stability of the evaluation of the GL ΔASL on a similar time span. Five successive trend evaluations were performed over an 11-year period (Fig. 6). Each evaluation is shifted with respect to the previous one by 1500 days. The results show large discrepancies, which could be associated with sudden sea level rise or fall (see Fig. 2). In the Northern group, the sea level rise observed at the end of 2013 (day count 7500 from the beginning of GL data) explains the larger trend observed in the fifth block (2009–2020 or day count 6000–10,000). The same phenomenon observed in the third block of GL data from Tubuai (2001–2012 or day count 3000–7000) is due to the sea level rise at the beginning of 2008 (day count 5500). The low value in Tubuai GL data (2009–2020, or days 6000–10,000) is mainly due to the sea level drop of 2012 (day count 7000). Moreover, the Northern group of stations exhibits opposite trend variations compared with the Southern group, with a correlation coefficient of −0.8. Inside the Northern group, the correlation reaches a value of 0.9 between the variations observed in Papeete/Vairao TGs on one side and Makemo/Rangiroa TGs on the other. Once more, the Northern and Southern

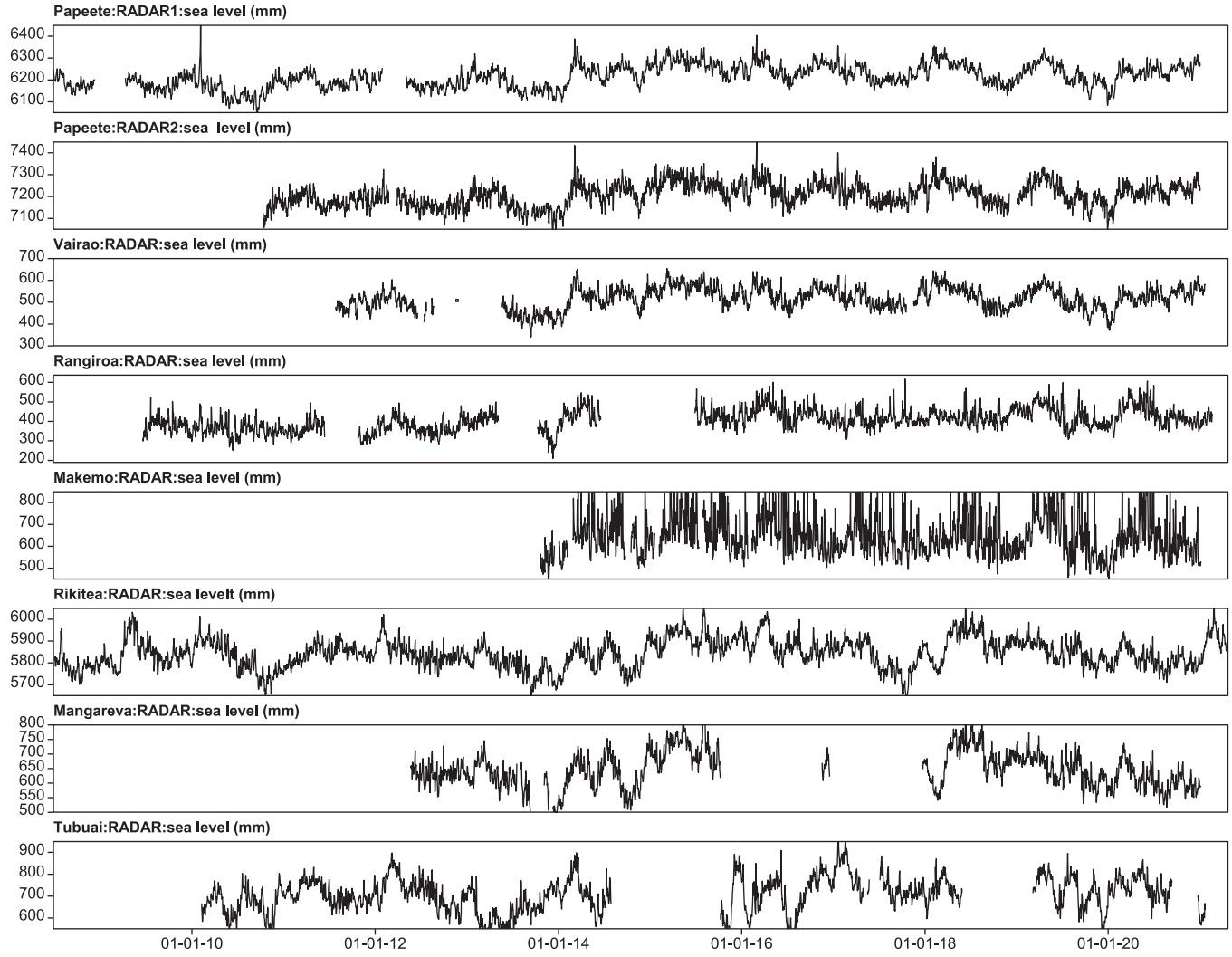

Fig. 3. Tide Gauge ΔRSL records in the same order as in Fig. 2, down-filtered to daily values. From top to bottom: Papeete (radar R1 and radar R2, see Table 1), Vairao, Rangiroa, Makemo, Rikitea, Mangareva, and Tubuai. A comparison between Fig. 2 and Fig. 3 clearly shows that Tide Gauge ΔRSL records in Makemo are strongly affected by the sea swell.

groups of stations display different but coherent behaviors. The conclusion is that an 11-year data set is too short to determine a reliable secular trend.

Generally, the secular trends (ΔASL), determined from the GL data on the time span they have in common with TG data (Table 4), do not align with the estimates from the 10,013 days of the whole GL data set (Table 3). Rikitea is the only station where the global GL estimation of the sea level trend (Table 3) agrees with the value computed on the same time span as the TG observations (Table 4).The determination of the ΔRSL from TG data over their available time span (always shorter than 5000 days) is therefore also questionable. More specifically, two stations pose problems: Makemo TG, where a large swell is present (Fig. 3), and Papeete TG, where sudden large sea level rises are showing up (Fig. 7). The first and largest one (from February 3–5, 2010) is related to the Oli cyclone, which passed close to the Society Islands (Barriot et al., 2016). It is a local phenomenon, as it does not show up in GL data. Another large sea level rise, of lower amplitudes, is also occurring at the beginning of February 2014. On the remaining stations, we first compared the secular trends estimated with TG and GL on the same time interval (Table 5). The difference should not exceed a mm/yr, considering the vertical displacements of the TG and the associated RMS errors. We see a good agreement between TG and GL results for the stations Vairao, Mangareva, and Rikitea, but not for Rangiroa and Tubuai. For these stations, the data set is split into several parts separated by large gaps (Fig. 3), due to long breakdowns in the instrumentation. A closer look showed that there is a jump in each station. To correct these offsets, we first subtracted the GL ΔASL data from the TG ΔRSL observations, according to the procedure implemented by Ray et al. (2023) for sea level records acquired on small islands, and that was successful in detecting offsets at the centimeter level. This differentiation removes the common low-frequency spectrum of the signals (Fig. 4). Thereafter, a step function was fitted to the differentiated data according to the procedure outlined in Van Camp and Vauterin (2005) and Ducarme et al. (2023). In total, we estimated the following drifts to be: 19.5 ± 1.1 mm in Rangiroa and 39.5 ± 2.4 mm in Tubuai. Once the drifts are corrected, we got similar trends for the TG ΔRSL and GL ΔASL data for these stations (Table 4).

As a direct determination of ΔRSL is not possible with a too short 11-year TG time series, we tried an alternative method, by combining ΔASL and VLM values (Eq. 1). It is indeed possible to determine a proxy of the VLM by a simple difference between GLORYS or altimeter data (ΔASL) and TG data (ΔRSL), as widely discussed in the literature (Wöppelmann and Marcos, 2016; Ray et al., 2023). It allows for the elimination of interannual variations in sea level, which are common to GL and TG data (Fig. 4), and to obtain results largely free of these effects. The drawback of the method is that it is based on the use of the model-assisted GL data

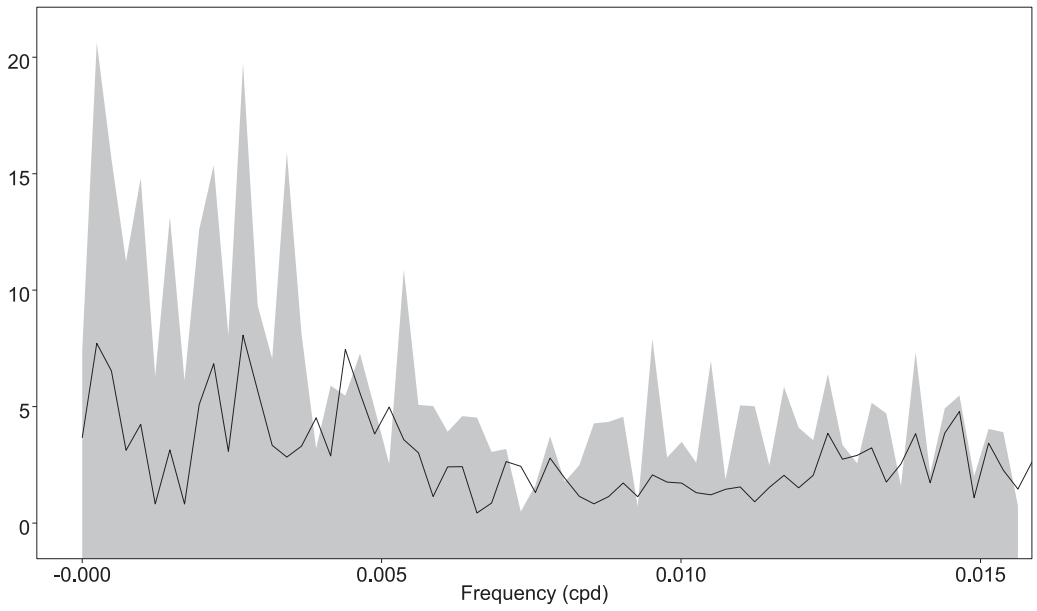

Fig. 4. Amplitude Fourier spectrum (in mm) for daily Vairao TG ΔRSL records (gray area) and of corresponding residues after subtraction of GL ΔASL data (black line), illustrating the large spectral correlation between the two datasets up to 0.014 cpd (periods larger than 70 days).

Table 2
Comparison of El Niño Southern Oscillation (ENSO) and GLORYS ΔASL spectra in the inter-annual spectrum of ENSO: MEI and NINO34 (Fig. 12 in Moreira et al. 2021). Northern group: Vairao, Rangiroa, and Makemo; and Southern group: Mangareva/Rikitea and Tubuai.

ENSO Period (year)	**Northern group** Period (year)	**Southern group** Period (year)	**Identification**	**ENSO** Frequency (cpd)
27	/	22.8	IPO	0.0001
10.8	11	11	PDO	0.00025
5.7	/	5.5	ENSO; PDO/2	0.00048
4.3	4	/	ENSO	0.00064
3.6	/	3.7	ENSO; PDO/3	0.00076
3	3	3	QBO1; ENSO	0.00091
2.4	2.5	/	QBO2; ENSO	0.00114

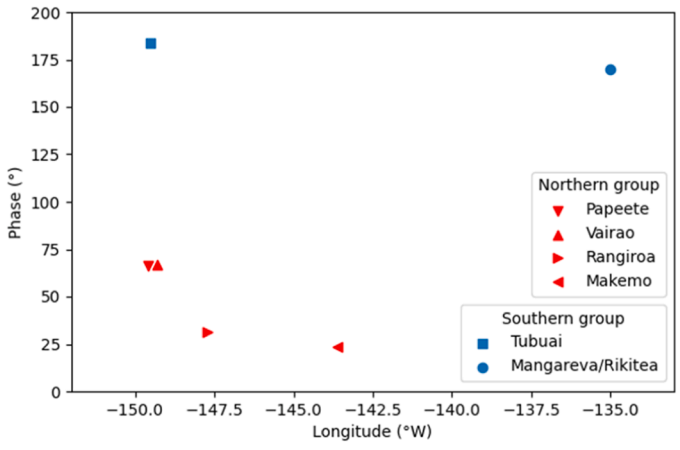

Fig. 5. Phase of the Pacific Decadal Oscillation (PDO) signal in GLORYS ΔASL data for Southern group Islands (Tubuai (149.5°W) and Mangareva/Rikitea (135°W)), Northern group (Papeete (149.6°W), Vairao (149.3°W), Rangiroa (147.7°W), and Makemo (143.5°W)).

set. The results are reported in Table 4. There is a good agreement

Table 3
Secular trends ΔASL_{GL} computed from GLORYS data and comparison with Li et al., (2024) results. Note that in option 2, several Long Period (LP) terms with periods up to 11 years are subtracted.

TG station	Option 1	Option 2		(Li et al. 2024) (mm/yr)
	slope (mm/yr)	slope (mm/yr)	Eliminated contribution of the LP terms (mm/yr)	
Papeete	1.90 ± 0.05	1.88 ± 0.05	0.02 ± 0.03	•2.8 ± 0.7
Vairao	1.79 ± 0.06	1.78 ± 0.05	0.03 ± 0.03	2.38 ± 0.03
Rangiroa	2.36 ± 0.04	2.33 ± 0.04	0.00 ± 0.02	2.30 ± 0.04
Makemo	2.26 ± 0.04	2.28 ± 0.04	-0.02 ± 0.02	2.32 ± 0.06
Riki/ Manga	2.28 ± 0.07	2.21 ± 0.07	-0.06 ± 0.02	2.13 ± 0.17
		*1.90 ± 0.07	*0.38 ± 0.02	
Tubuai	3.91 ± 0.08	3.81 ± 0.08	-0.04 ± 0.03	3.82 ± 0.11
		*2.63 ± 0.08	*1.28 ± 0.02	

• Value from (Becker et al., 2012). * After additional subtraction of the 23.5-year IPO signal

between the VLM proxies and the VLM values deduced from the GPS observations (Table 4), proving that VLM estimation through Eq. (2) is reliable.

Papeete TG deserves special attention (Table 5). Initially, the VLM estimates from radar R1 (−1.46 ± 0.30 mm/yr) and radar R2 (−1.87 ± 0.20 mm/yr) data seemed quite different (see Table 1). However, when we discard the large perturbation in R1 records at the beginning of February 2010 (cyclone Oli, Fig. 7), we obtain a value of −1.91 ± 0.20 mm/yr, close to the R2 value. Comparison of our results with the values given by Ray et al. (2023), Table 5) shows some discrepancies when TG ΔRSL values are calculated on different time periods. This reveals the presence of inflection points in the VLM proxy (Fig. 7). Our VLM estimates could be compared with the Global Navigation Satellite

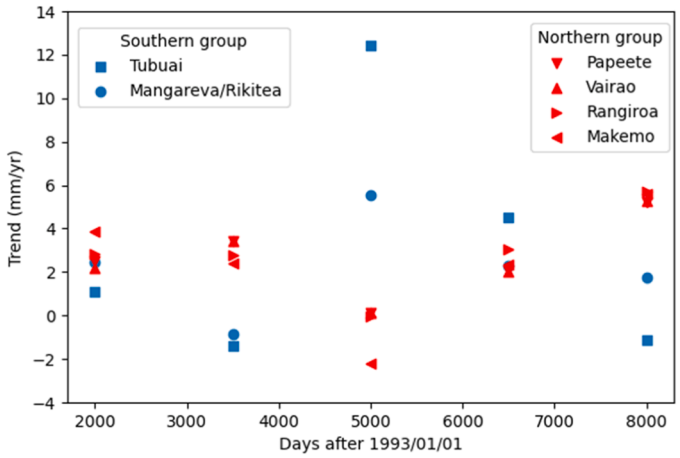

Fig. 6. Variations of the computed trend on 4000-days (11-years) subsets of GLORYS ΔASL data: Southern group (Mangareva/Rikitea and Tubuai), Northern group (Papeete, Vairao, Rangiroa, and Makemo). A correlation coefficient of −0.8 is observed between the variations of the two groups.

Table 4
Comparison of ΔRSL_{TG} with ΔASL_{GL} (columns 3 and 4) and of Vertical Land Motion (VLM) proxies from Tide Gauges (TG) or GLORYS (GL) with VLM estimates from Li et al. (2024) data (columns 5 and 6).

Station	Time span (days)	TG ΔRSL slope (mm/yr)	GL ΔASL slope (mm/yr)	VLM_{TG} = -(TG-GL) slope (mm/yr)	VLM_{GPS} slope (mm/yr)
Papeete R1	4357	6.42 ± 0.30	5.46 ± 0.13	-1.91 ± 0.20	PAPE[a] −1.61 ± 0.32
Papeete R2	3522	6.15 ± 0.30	5.70 ± 0.18	-1.87 ± 0.24	/
Vairao	3236	2.94 ± 0.33	3.04 ± 0.27	-0.37 ± 0.22	-0.49 ± 0.39
Rangiroa	4000	7.93 ± 0.25	/	/	/
Rangiroa*		5.12 ± 0.25	5.24 ± 0.17	0.11 ± 0.24	/
Mangareva	2933	3.83 ± 0.47	3.63 ± 0.40	-0.34 ± 0.50	-0.43 ± 0.17
Rikitea	4352	2.86 ± 0.27	2.20 ± 0.22	-0.55 ± 0.12	-0.43 ± 0.17
Tubuai	3767	5.23 ± 0.51	/	/	/
Tubuai**		-0.12 ± 0.52	-1.06 ± 0.35	-0.80 ± 0.28	-0.92 ± 0.17

* With 19.5 ± 1.10 mm offset correction **With 39.5 ± 2.38 mm offset correction
[a] (Blewitt et al. 2016) in Table 5

Systems (GNSS) result at the International GNSS Service (IGS) station PAPE (Table 5, coordinates 17.533°S, 149.573°W) collocated with the TG. There is a good agreement with Blewitt et al., (2016) and Heflin et al., (2020). However, a more recent result (Gravelle et al., 2023) provides much smaller VLM estimates (-0.98 mm/year) on a data set extending up to 21.7 years, illustrating also the time dependence of the VLM estimates at IGS station PAPE.

It should be noted that another IGS GPS station, THTI (17.577°S, 149.606°W, Geodesy Observatory of Tahiti), used by other sources (SONEL, 2022; Li et al., 2024) is located 6 km away uphill (100 m altitude) from the IGS GPS station PAPE. The THTI VLM value from Li et al. (2024) −0.74 ± 0.10 mm/yr agrees with the most recent VLM estimates from more than 20 years of observations: −0.93 ± 0.66 mm/yr (NGL, 2022) and −0.82 ± 0.10 mm/yr (ITRF2020, 2022) and with the new IGS station PAPE value −0.98 mm/yr (Gravelle et al., 2023).

The VLM proxies from stations Vairao TG and Papeete TG agree with the GPS observations and confirm the lower ΔASL values of the GL grid for the Society Archipelago.

In the final step, we estimated the corresponding ΔRSL trends by subtracting VLM values from ΔASL values. Table 6 reports the trends (ΔRSL1) extracted from Li et al. (2024) and the trends (ΔRSL2) from this study. At Vairao, the ΔRSL2 trend is lower than the ΔRSL1 trend due to the low value of ΔASL_{GL}. ΔRSL2 trend estimated at Rikitea TG agrees with the trend directly computed from TG ΔRSL observations (Table 4). It is not surprising, since Rikitea TG is the only station where the global GL ΔASL estimation of the sea level trend (Table 3) agrees with the value computed on the same time interval as the TG observation (Table 4). At Tubuai, the IPO corrected ΔASL_{GL} value (2.63 ± 0.08 mm/yr.) provides the value ΔRSL2 = 3.43 ± 0.29 mm/yr. In Rikitea also the secular trend ΔRSL2 is only 2.45 ± 0.14 mm/yr, after correction of the IPO contribution. To have a realistic estimate of the ΔRSL2 value, in Tubuai it is necessary to add to the secular trend the IPO signal, with an amplitude of 31.1 ± 1.6 mm and a maximum in August 2012. At the peak of the IPO, the sea level rises by 3 cm relative to the calculated secular trend. This could disturb the determination of sea level acceleration related to global warming.

At Papeete station, different ΔRSL1 trends are obtained depending on different time spans (Li et al., 2024, Table 6). The recent VLM_{PAPE} value of −0.98 mm/year (Gravelle et al., 2023) associated with the ΔASL_{GL} value provides a ΔRSL2 value of 2.86 mm/year, much closer to the Vairao value. This confirms that the tide gauge measurements at Papeete station are strongly disturbed, probably due to its location deep in the harbor, and do not provide reliable VLM_{TG} or ΔRSL values.

5. Discussion and Conclusions

The analysis of 27.5 years of GL data reveals a contrast between a Northern group of TG stations (the Society Islands, with Papeete and Vairao, and the Tuamotu Archipelago, with Rangiroa and Makemo) and a Southern group of TG stations (the Gambier Islands with Mangareva/Rikitea and Tubuai in the Austral Islands). A strong decrease in the spectral amplitude of sea surface records is observed at 0.003 cpd for the Northern group and at 0.0125 cpd for the Southern group. This difference in spectral content is the reason why we can create these two groups. The inter-annual signal associated with ENSO is visible everywhere, as well as the PDO signal of the 11-year period, which is present everywhere. However, the PDO from the Northern group is in phase opposition with the PDO from the Southern group. The IPO is only present in the Southern group, with a spectral peak at 23.5 years.

Different computation methods have been proposed to determine the ΔASL secular trend from the GL data set. The contributions of the sea level variability, with periods lower than 20 years, are negligible on the 27.5 years GL ΔASL. Their contribution is lower than 0.05 mm/yr. This is not the case of the 23.5-year IPO signal in Tubuai and Rikitea. The large secular trend value found in Tubuai (3.81 ± 0.08 mm/yr) is largely explained by the IPO. The secular trend is reduced to 2.63 ± 0.08 mm/yr after elimination of several very long period waves, including the IPO. They account for a 1.28 ± 0.02 mm/yr trend. In Rikitea the elimination of IPO reduces the secular trend ΔASL_{GL} from 2.21 ± 0.07 mm/yr to 1.89 ± 0⊡07 mm/yr. The available time span of the GL data is obviously too short to extract a reliable secular trend ΔASL for the Southern group of stations. Our results are in overall agreement with the results of Li et al. (2024), except for Papeete and Vairao (Society Islands) TGs, where the ΔASL_{GL} value is lower.

On a shorter time span (4000 days or 11 years), the determination of the secular trend in GL ΔASL is unstable due to the strong oscillations of the sea level at this scale. The Northern group exhibits opposite variations compared with the Southern group. The trends estimated for the TG ΔRSL data agreed with the GL ΔASL data on the same time span, except in Rangiroa and Tubuai. Subtracting GL ΔASL data from TG ΔRSL data was a powerful tool to detect offset in TG ΔRSL data and allowed us

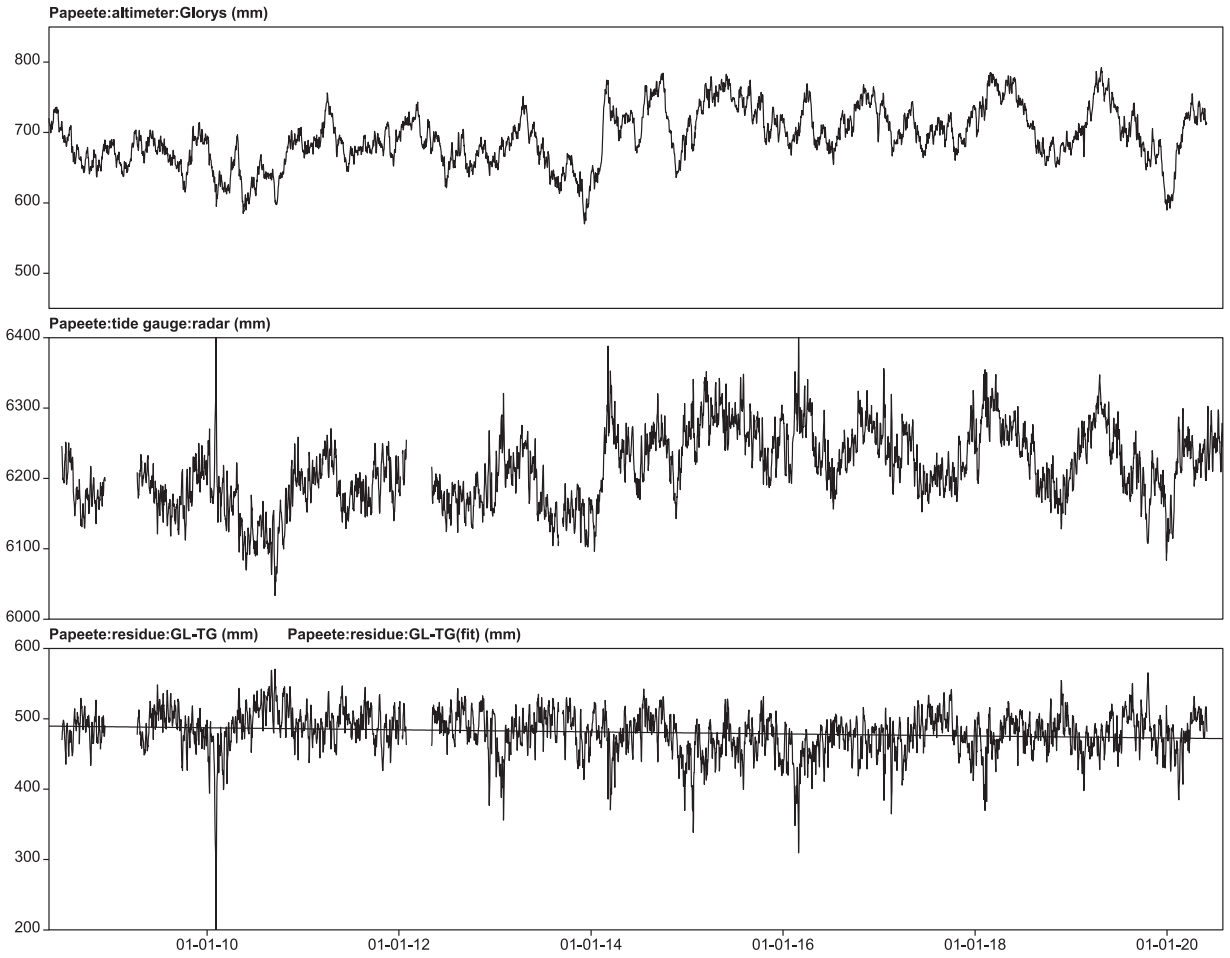

Fig. 7. Summary of results at Tide Gauge (TG) station Papeete. Top to bottom: GLORYS (GL), middle: radar R1 (TG), bottom: VLM_{TG}= (GL-TG), should be compared to Ray et al. (2023), Fig. 8. The large peak on TG data at the beginning of the year 2010 corresponds to the Oli cyclone.

Table 5
Comparison of different Vertical Land Motion (VLM) estimates at International GNSS Service (IGS) station Papeete (PAPE). Results at the IGS THTI station are given for comparison purposes. GPS coordinates: PAPE (17.533°S, 149.570°W), THTI (15.577°S,149.606°W).

VLM_{TG} at PAPE (mm/yr)					VLM GNSS (mm/yr)			
(Ray et al. 2023)			This study		UNR[a]	JPL[2]	ULR[3]	(Li et al. 2024)
1993–2007	**2008–2018**	**1993–2018**	**R1**	**R2**	**PAPE**	**PAPE**	**PAPE**	**THTI**
			2008–2020	**2010–2020**				
-1.70 ± 0.48	-2.25 ± 0.60	-1.90 ± 0.37	-1.91 ± 0.20	-1.87 ± 0.24	-1.61 ± 0.32	-1.57 ± 0.77	-0.98	-0.74 ± 0.10

[a] (Blewitt et al. 2016), [2](Heflin et al. 2020), [3](Gravelle et al., 2023). See also Santamaría-Gómez et al. (2025).

to correct jumps inside these two data sets.

As the direct determination of ΔRSL is not possible with the available 11-year TG time series, we tried an alternative method, by combining ΔASL and VLM values. The secular trend computed after subtraction of the GL ΔASL data from the TG ΔRSL data is a proxy of the VLM (changed of sign). We have an excellent agreement with the GPS VLM estimates available at the 3 UPF (University of French Polynesia) TG stations, i.e. Vairao, Mangareva/Rikitea, and Tubuai. It is proof of the reliability of the recorded TG data in French Polynesia. The UH (University of Hawaii) station Papeete (PAPE), studied by Ray et al. (2023), is a special case, as the VLM proxy values depend on the length of the series. These might be due to the existence of inflection points in the GL ΔASL minus TG ΔRSL curve. Our VLM determination agrees with the GPS results, also at IGS station PAPE (Papeete harbor). This result confirms the lower ΔASL values obtained from the GL grid for the Society Islands.

As an update on the risks of possible long-term sea submersion in coastal areas of French Polynesia, we reconstructed the ΔRSL trends (Table 6) at six TGs stations (Table 1 and Fig. 1) distributed over French Polynesia either from the ΔASL and VLM results of Li et al. (2024) or from the combination of the secular trends in the GL data (ΔASL) and the VLM values deduced from the differences ΔASL_{GL} - ΔRSL_{TG}. There is a good agreement between the two methods, except at Papeete and Vairao TGs. It is due to the lower ΔASL value deduced from the GL data. Values around 2.2 mm/yr are obtained at Vairao and Rangiroa. At Papeete, different ΔRSL trends are obtained according to different time spans, ranging from 2.62 ± 0.39 mm/yr to 3.20 ± 0.40 mm/yr. A recent VLM value (Gravelle et al., 2023) provides a ΔRSL value of 2.86 mm/yr. In the Southern group of stations, the IPO modulates the long-term sea-level variation with an amplitude reaching 3 cm at Tubuai. It stresses the fact that very long term interannual sea level variations can affect the coastal risk assessment and perturb the evaluation of the sea level rise due to the global warming. After correction of the IPO contribution, we get 2.45 ± 0.14 mm/yr at Rikitea and 3.43 ± 0.29 mm/yr at Tubuai.

Table 6
Evaluation of ΔRSL= ΔASL-VLM trends at Tide Gauge stations Papeete, Varirao, Rangiroa, Rikitea/Mangareva (Riki/Manga), and Tubuai.

Station	*(Li et al., 2024) (mm/yr.)			This study (mm/yr.)		
	ΔASL_{LI}	VLM_{LI}	ΔRSL1	ΔASL_{GL}	VLM_{TG}	ΔRSL2
Papeete (PAPE)	/	/	From 2.62 ± 0.39–3.20 ± 0.40*	1.88 ± 0.05	-1.89 ± 0.22 **	3.77 ± 0.23
Vairao	2.38 ± 0.03	-0.49 ± 0.39	2.87 ± 0.39	1.78 ± 0.05	-0.37 ± 0.22	2.15 ± 0.23
Rangiroa	2.30 ± 0.04	/	/	2.33 ± 0.04	0.11 ± 0.24	2.22 ± 0.24
Riki/ Manga	2.13 ± 0.17	-0.43 ± 0.17	2.56 ± 0.24	2.21 ± 0.07 ***	-0.55 ± 0.12	2.76 ± 0.14
Tubuai	3.82 ± 0.11	-0.92 ± 0.17	4.74 ± 0.20	3.81 ± 0.08 ***	-0.80 ± 0.28	4.61 ± 0.29

* Adapted from Li et al. (2024), Table 6.
** Adoption of the Gravelle et al. VLM value −0.98 mm/yr, would reduce ΔRSL2–2.86 mm/yr.
*** Including the IPO signal (Table 3). Subtraction of the inter-annual variability reduces ΔRSL2 to –2.45 ± 0.14 mm/yr (Riki/Manga) and 3.43 ± 0.29 (Tubuai).

CRediT authorship contribution statement

Bernard Ducarme: Writing – review & editing, Writing – original draft, Visualization, Validation, Methodology, Investigation, Formal analysis, Data curation, Conceptualization. **Marania Hopuare:** Writing – review & editing, Data curation. **Jean-Pierre Barriot:** Writing – review & editing, Supervision, Resources, Project administration, Funding acquisition, Conceptualization. **Xianjie Li:** Writing – review & editing, Visualization. **Keitapu Maamaatuaiahutapu:** Writing – review & editing.

Declaration of Competing Interest

The authors declare that they have no known competing financial interests or personal relationships that could have appeared to influence the work reported in this paper.

Acknowledgements

The Geodesy Observatory of Tahiti thanks the French Space Agency (CNES) for support through a "Decision d'Aide à la Recherche" annual funding, as well as continuous support from the University of French Polynesia, the authorities of French Polynesia, and the Hydrographic Service of the French Navy (SHOM).

Data availability

Data will be made available on request.

References

Adebisi, N., Balogun, A.L., Min, T.H., Tella, A., 2021. Advances in estimating sea level rise: a review of tide gauge, satellite altimetry, and spatial data science approaches. Ocean Coast Manag 208, 105632. https://doi.org/10.1016/j.ocecoaman.2021.105632.

Albrecht, F., Pizarro, O., Montecinos, A., Zhang, X., 2019. Understanding sea level change in the South Pacific during the late 20th century and early 21st century. J. Geophys Res Ocean 124, 3849–3858. https://doi.org/10.1029/2018JC014828.

Ansari, K., 2025. Extended Kalman Filter analysis of sea-level changes along the Black Sea coast and comparison with satellite altimetry. Discov. Geosci. 3 (194), 1–12. https://doi.org/10.1007/s44288-025-00316-1.

Ansari, K., Walo, J., Wezka, K., Biswas, M., Mukherjee, S., 2024. Regional tidal modelling at European coast using tide gauges and satellite altimetry, 1412736 Front. Mar. Sci. 11, 1–14. https://doi.org/10.3389/fmars.2024.1412736.

Barriot, J.-P., Serafini, J., Maamaatuaiahutapu, K., Sichoix, L., 2016. The Island of Tubuai (French Polynesia) landfall of cyclone Oli on the 5th of February 2010. Open Access Libr. J. 03, 1–9. https://doi.org/10.4236/oalib.1102615.

Barriot, J.P., Zhang, F., Ducarme, B., et al., 2023. A database for sea-level monitoring in French Polynesia. Geosci. Data J. 10, 368–384. https://doi.org/10.1002/gdj3.172.

Becker, M., Meyssignac, B., Letetrel, C., et al., 2012. Sea level variations at tropical Pacific islands since 1950. Glob. Planet Change 80–81, 85–98. https://doi.org/10.1016/j.gloplacha.2011.09.004.

Blewitt, G., Kreemer, C., Hammond, W.C., Gazeaux, J., 2016. MIDAS robust trend estimator for accurate GPS station velocities without step detection. AGU J. Geophys Res Solid Earth 121, 2054–2068. https://doi.org/10.1002/2015JB012552.

Cazenave, A., Dominh, K., Ponchaut, F., et al., 1999. Sea level changes from Topex-Poseidon altimetry and tide gauges, and vertical crustal motions from DORIS. Geophys Res Lett. 26, 2077–2080. https://doi.org/10.1029/1999GL900472.

CMEMS (2024a). Global Ocean Physics Reanalysis products GLORYS12V1. In: Mar. Data Store.

CMEMS (2024b). Global Ocean Gridded L4 Sea Surface Heights and Derived Variables Reprocessed 1993 Ongoing. In: Mar. Data Store.

Dai, A., 2013. The influence of the inter-decadal Pacific oscillation on US precipitation during 1923-2010. Clim. Dyn. 41, 633–646. https://doi.org/10.1007/s00382-012-1446-5.

Dai, A., Fyfe, J.C., Xie, S.P., Dai, X., 2015. Decadal modulation of global surface temperature by internal climate variability. Nat. Clim. Chang 5, 555–559. https://doi.org/10.1038/nclimate2605.

Dong, B., Dai, A., 2015. The influence of the Interdecadal Pacific Oscillation on Temperature and Precipitation over the Globe. Clim. Dyn. 45, 2667–2681. https://doi.org/10.1007/s00382-015-2500-x.

Ducarme, B., Barriot, J.P., Zhang, F., 2023. Combination of Tsoft and ET34-ANA-V80 software for the preprocessing and analysis of tide gauge data in French Polynesia. Geod. Geodyn. 14, 26–34. https://doi.org/10.1016/j.geog.2022.05.002.

Dunkerton, T.J., 2003. MIDDLE ATMOSPHERE | Quasi-Biennial Oscillation. Encycl. Atmos. Sci. 1328–1336. https://doi.org/10.1016/b0-12-227090-8/00232-3.

Fadil, A., Sichoix, L., Barriot, J.P., et al., 2011. Evidence for a slow subsidence of the Tahiti Island from GPS, DORIS, and combined satellite altimetry and tide gauge sea level records. Comptes Rendus - Geosci. 343, 331–341. https://doi.org/10.1016/j.crte.2011.02.002.

Fyfe, J.C., Meehl, G.A., England, M.H., et al., 2016. Making sense of the early-2000s warming slowdown. Nat. Clim. Chang 6, 224–228. https://doi.org/10.1038/nclimate2938.

Gravelle, M., Wöppelmann, G., Gobron, K., Altamimi, Z., Guichard, M., Herring, T., Rebischung, P., 2023. The ULR-repro3 GPS data reanalysis and its estimates of vertical land motion at tide gauges for sea level science. Earth System Science. Data 15 (1), 497–509. https://doi.org/10.5194/essd-2022-23.

Gu, G., Adler, R.F., 2015. Spatial patterns of global precipitation change and variability during 1901-2010. J. Clim. 28, 4431–4453. https://doi.org/10.1175/JCLI-D-14-00201.1.

Hamlington, B.D., Strassburg, M.W., Leben, R.R., et al., 2014. Uncovering an anthropogenic sea-level rise signal in the Pacific Ocean. Nat. Clim. Chang 4, 782–785. https://doi.org/10.1038/nclimate2307.

He, X., Huang, J., Montillet, J.P., Wang, S., Kermarrec, G., Shum, C.K., Hu, S., Wang, F., 2025. A noise reduction approach for improve North American regional sea level change from satellite and In Situ observations. Surv. Geophys. 1–32. https://doi.org/10.1007/s10712-025-09894-8.

Heflin, M., Donnellan, A., Parker, J., et al., 2020. Automated estimation and tools to extract positions, velocities, breaks, and seasonal terms from daily GNSS measurements: illuminating nonlinear Salton trough deformation. Earth Sp. Sci. 7. https://doi.org/10.1029/2019EA000644.

Hopuare, M., Pontaud, M., Céron, J.P., et al., 2015. Climate change, Pacific climate drivers, and observed precipitation variability in Tahiti, French Polynesia. Clim. Res 63, 157–170. https://doi.org/10.3354/cr01288.

Hua, W., Dai, A., Qin, M., 2018. Contributions of internal variability and external forcing to the recent pacific decadal variations. Geophys Res Lett. 45, 7084–7092. https://doi.org/10.1029/2018GL079033.

Huppert, K.L., Perron, J.T., Royden, L.H., 2020. Hotspot swells and the lifespan of volcanic ocean islands. Sci. Adv. 6 (1), 1–9. https://doi.org/10.1126/sciadv.aaw6906.

IERS ITRS Center (2022). ITRF2020. ⟨https://itrf.ign.fr/en/solutions/ITRF2020⟩. Accessed 8 Sep 2024.

Kosaka, Y., Xie, S.P., 2013. Recent global-warming hiatus tied to equatorial Pacific surface cooling. Nature 501, 403–407. https://doi.org/10.1038/nature12534.

Kuo, C.Y., Shum, C.K., Braun, A., Mitrovica, J.X., 2004. Vertical crustal motion determined by satellite altimetry and tide gauge data in Fennoscandia. Geophys Res Lett. 31. https://doi.org/10.1029/2003GL019106.

Lellouche, J.-M., Greiner, E., Badie-Bourdallé, R., et al., 2021. The Copernicus Global 1/12° Oceanic and Sea Ice GLORYS12 Reanalysis. Front Earth Sci. 9, 698876.

Li, X., Barriot, J.P., Ducarme, B., et al., 2024. Monitoring absolute vertical land motions and absolute sea-level changes from GPS and tide gauge data over French Polynesia. Geod. Geodyn. 15, 13–26. https://doi.org/10.1016/j.geog.2023.02.007.

Mantua, N.J., 2003. Pacific–Decadal Oscillation (PDO). In: Munn, T. (Ed.), Encyclopedia of Global Environmental Change, 1st ed. John Wiley & Sons, Chichester, England, pp. 592–594.

Martinez, E., Ganachaud, A., Lefevre, J., Maamaatuaiahutapu, K., 2009. Central South Pacific thermocline water circulation from a high-resolution ocean model validated against satellite data: Seasonal variability and El Nin˜o 1997 – 1998 influence. J. Geophys. Res. 114, C05012. https://doi.org/10.1029/2008JC004824.

Martínez-Asensio, A., Wöppelmann, G., Ballu, V., Becker, M., Testut, L., Magnan, A.K., Duvat, V.K.E., ISSN 0921-8181, 2019. Relative sea-level rise and the influence of vertical land motion at Tropical Pacific Islands. Glob. Planet. Change 176, 132–143. https://doi.org/10.1016/j.gloplacha.2019.03.008.

Moreira, L., Cazenave, A., Palanisamy, H., 2021. Influence of inter-annual variability in estimating the rate and acceleration of present-day global mean sea level. Glob. Planet Change 199. https://doi.org/10.1016/j.gloplacha.2021.103450.

NGL (2022) Station Page for THTI. ⟨http://geodesy.unr.edu/NGLStationPages/stations/THTI.sta⟩. Accessed 8 Sep 2024.

Oelsmann, J., Marcos, M., Passaro, M., et al., 2024. Regional variations in relative sea-level changes influenced by nonlinear vertical land motion. Nat. Geosci. 17, 137–144. https://doi.org/10.1038/s41561-023-01357-2.

Pagli, B., Izumo, T., Cravatte, S.E., Hopuare, M., Martinoni-Lapierre, S., Laurent, V., Auffray, S., 2025. The diverse impacts of El Niño and La Niña events over the South Pacific and in French Polynesia. J. Clim. 38 (12), 2681–2701.

Power, S., Casey, T., Folland, C., et al., 1999. Inter-decadal modulation of the impact of ENSO on Australia. Clim. Dyn. 15, 319–324. https://doi.org/10.1007/s003820050284.

Ray, R.D., Widlansky, M.J., Genz, A.S., Thompson, P.R., 2023. Offsets in tide-gauge reference levels detected by satellite altimetry: ten case studies. J. Geod. 97. https://doi.org/10.1007/s00190-023-01800-7.

Salinger, M.J., Renwick, J.A., Mullan, A.B., 2001. Interdecadal Pacific Oscillation and South Pacific climate. Int J. Clim. 21, 1705–1721. https://doi.org/10.1002/joc.691.

Santamaría-Gómez, A., Boy, J.P., Feriol, F., Gravelle, M., Loyer, S., Nahmani, S., Nicolas, J., García Pallero, J.L., Panetier, A., Pollet, A., Sakic, P., 2025. Monitoring the Earth's deformation with the SPOTGINS series. Earth Syst. Sci. Data 17 (11), 5833–5840.

Schüller, K., 2015. Theoretical basis for earth tide analysis with the new ETERNA34-ANA-V4.0 program. Bull. D. 'Inf. Des. Marees Terr. 149, 12024–12061.

Schüller K. (2017) ETERNA-x – Earth Tide Analysis and Prediction Program. ⟨https://eterna.bkg.bund.de/⟩. Accessed 20 Oct 2024.

SONEL (2022) GPS TAHITI. ⟨https://www.sonel.org/?page=gps&idStation=852⟩. Accessed 8 Sep 2024.

Van Camp, M., Vauterin, P., 2005. Tsoft: Graphical and interactive software for the analysis of time series and Earth tides. Comput. Geosci. 31, 631–640. https://doi.org/10.1016/j.cageo.2004.11.015.

Wöppelmann, G., Marcos, M., 2012. Coastal sea level rise in southern Europe and the nonclimate contribution of vertical land motion. J. Geophys Res Ocean 117. https://doi.org/10.1029/2011JC007469.

Wöppelmann, G., Marcos, M., 2016. Vertical land motion as a key to understanding sea level change and variability. Rev Zhang Y, Wallace JM, Battisti DS (1997) ENSO-like interdecadal variability: 1900-93. J. Clim. 10, 1004–1020. https://doi.org/10.1175/1520-0442(1997)010<1004:eliv>2.0.co;2.

Zhang, Y., Wallace, J.M., Battisti, D.S., 1997. ENSO-like Interdecadal Variability: 1900–93. J. Climate 10, 1004–1020. https://doi.org/10.1175/1520-0442(1997)0102.0.CO;2.